DALTON
FULL PAPER

Homoleptic complexes of Ag(I), Cu(I), Pd(II) and Pt(II) with tetrathiafulvalene-functionalized phosphine ligands †

Bradley W. Smucker and Kim R. Dunbar *

Department of Chemistry, Texas A&M University, PO Box 30012, College Station, TX 77842-3012, USA

Received 27th October 1999, Accepted 22nd February 2000
Published on the Web 31st March 2000

Homoleptic complexes of the type $[M(L–L)_2]^{+/2+}$ where L–L is a chelating tetrathiafulvalene-based phosphine ligand have been synthesized and fully characterized by X-ray crystallography, $^{31}P\{^1H\}$ NMR spectroscopy and electrochemistry. In this study, square-planar cations of Pd(II) and Pt(II) with tetrakis(diphenylphosphino)-tetrathiafulvalene (P4) and tetrahedral cations of Ag(I) and Cu(I) with 3,4-dimethyl-3′,4′-bis(diphenylphosphino)-tetrathiafulvalene (o-P2) have been isolated. X-Ray studies of six different crystalline compounds revealed that the conformation of the TTF (tetrathiafulvalene) substituents is highly influenced by crystal packing forces. As judged by the remarkable similarity of each Pd/Pt or Cu/Ag pair, the solid-state structures are independent of the identity of the metal. Electrochemical studies indicate that the TTF redox centers on the different phosphine ligands are electronically isolated in these compounds.

In the past two decades, synthetic chemists have endeavored to prepare molecule-based materials with tunable conducting, magnetic or optical properties.[1–4] These goals have largely been treated as separate efforts in the organic and inorganic communities, but recently it has become apparent that exciting prospects for materials chemistry exist at the interface of the two areas.[3] An excellent example of this point is the discovery of superconducting charge-transfer salts composed of bis(ethylenedithio)TTF (BEDT-TTF) radicals and paramagnetic metal-based anions.[4] This finding has paved the way for a new field of dual-property materials that are capable of behaving as both conductors and magnets.

In addition to co-assembling organic donors and metal anions, another strategy for constructing inorganic/organic "hybrids" is the direct coordination of paramagnetic metals to organic radicals through an intervening heteroatom.[1,5] In considering possible candidates to act as organic linkers in such compounds, we turned to redox-active ligands that are likely to form strong metal interactions enhanced by chelation (Fig. 1).[6–9] The choice of tertiary phosphines is a natural one, as they are known for stabilizing transition metals in a wide range of oxidation states,[10] and for being relatively easy to modify with respect to electronic and steric effects. Furthermore, the ability to chelate or bridge increases the stability of the metal compounds through the formation of five- or six-membered rings. The addition of a redox active substituent is of additional interest for subtle tuning of metal center electron density (and consequently reactivity) by addition or removal of an electron from the ligand.[11] Such flexibility allows for control of the stability, catalytic properties, and chemical selectivity of metal complexes, to name a few of the most prominent applications.[12]

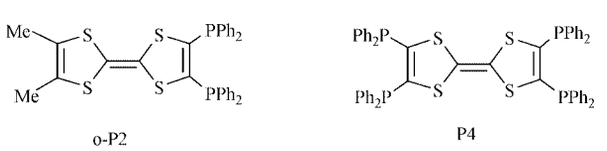

Fig. 1 Schematic drawings of phosphine ligands based on tetrathiafulvalene.

† Dedicated to Professor F. Albert Cotton on the occasion of his 70th birthday.

In this paper, we report the isolation and characterization of homoleptic square planar, $[M(P4)_2][BF_4]_2$ (Pd, **1** and Pt, **2**), and tetrahedral, $[M(o\text{-}P2)_2][BF_4]$ (Ag, **3** and Cu, **4**), compounds. The results of solution and solid-state studies aimed at understanding the electronic and steric issues that are operative in compounds of these ligands are discussed.

Results and discussion

Syntheses

$[M(P4)_2][BF_4]_2$ (M = Pd (1); Pt (2)). The P4 ligand contains *trans* binding sites that can be used to join metals in oligomeric arrays, a fact that led us to investigate 1 : 1 reactions of P4 with the labile starting materials $[M(CH_3CN)_{4–6}][BF_4]_2$ (M = Ni, Pd, Pt, Fe, Co).[7,8] In the course of investigating this chemistry, we discovered that products obtained in acetonitrile exhibit a single ^{31}P NMR resonance, which is indicative of a structure that does not contain phosphorus end groups.[9] Numerous attempts to characterize these soluble products were made; these include mass spectrometry, $^{31}P\{^1H\}$ NMR spectroscopy, cyclic voltammetry, and the formation of derivatives with capping ligands. Unfortunately, in the absence of single crystal X-ray data, one cannot draw any definitive conclusions about the structures of these compounds. To gain more insight into the nature of these products, we prepared the simplest entity of the oligomer, $\{[M(P4)][BF_4]_2\}_n$, namely the mononuclear derivative with two dangling P4 ligands. To accomplish this, a suspension of $[M(CH_3CN)_4][BF_4]_2$ (M = Pd, Pt) in CH_2Cl_2 was treated with an excess of P4 in CH_2Cl_2 which led to the production of a brown (Pd) or red (Pt) solution.[13] Excess P4 was removed by washing the crude solids with hot toluene. After work-up, $^{31}P\{^1H\}$ NMR spectra of the products in CH_2Cl_2 revealed two resonances, *viz*., one for coordinated phosphine groups (Pd = 41.7 ppm, Pt = 32.6 ppm, $J_{Pt–P}$ = 2401 Hz) and one attributable to unbound phosphine at −18.0 ppm. Brown (Pd) and red (Pt) crystals of the salts suitable for single crystal X-ray analysis were grown by slow diffusion of hexanes or toluene into CH_2Cl_2 solutions of $[M(P4)_2][BF_4]_2$. These conditions led

DOI: 10.1039/a908559i

Table 1 Crystal data and details of data collection and structural refinement for **1a**, **1b**, **2a**, **2b**, **3**·1.68(CH_3CN)·0.24(CH_2Cl_2) and **4**·2(CH_3CN)

	1a	**1b**	**2a**	**2b**	**3**·1.68(CH_3CN)·0.24(CH_2Cl_2)	**4**·2(CH_3CN)
Empirical formula	$C_{108}H_{80}B_2F_8P_8PdS_8$·4($CH_2Cl_2$)	$C_{108}H_{80}B_2F_8P_8PdS_8$·2($CH_2Cl_2$)·4($C_7H_8$)	$C_{108}H_{80}B_2F_8P_8PtS_8$·4($CH_2Cl_2$)	$C_{108}H_{80}B_2F_8P_8PtS_8$·2($CH_2Cl_2$)·4($C_7H_8$)	$C_{64}H_{52}AgBF_4P_4S_8$·1.68(CH_3CN)·0.24(CH_2Cl_2)	$C_{64}H_{52}CuBF_4P_4S_8$·2(CH_3CN)
M/g mol^{-1}	2501.68	2700.47	2590.38	2789.13	1486.07	1433.88
Crystal size/mm^{-1}	0.15 × 0.03 × 0.11	0.13 × 0.10 × 0.03	0.13 × 0.18 × 0.15	0.15 × 0.59 × 0.10	0.44 × 0.28 × 0.31	0.31 × 0.26 × 0.18
Crystal system	Monoclinic	Monoclinic	Monoclinic	Monoclinic	Monoclinic	Monoclinic
Space group	$P2_1/c$ (no. 14)	$C2/m$ (no. 12)	$P2_1/c$ (no. 14)	$C2/m$ (no. 12)	$P2_1/n$ (no. 14)	$P2_1/n$ (no. 14)
a/Å	17.0665(8)	22.527(4)	17.109(3)	22.540(4)	25.569(5)	17.788(4)
b/Å	19.0941(9)	16.736(3)	19.069(4)	16.739(3)	21.376(4)	20.676(4)
c/Å	19.2877(10)	17.944(3)	19.339(4)	17.929(4)	27.209(5)	18.183(4)
β/°	115.138(1)	112.40(3)	115.17(3)	112.35(3)	112.75(3)	90.83(3)
Volume/Å^3	5690.0(5)	6255(2)	5710.0(5)	6256(2)	13714(5)	6687(2)
Z	2	2	2	2	8	4
μ/mm^{-1}	0.671	0.534	1.735	1.507	0.702	0.727
Reflections collected	63739	26077	31256	19638	159669	33921
Unique reflections	13718 [R_{int} = 0.0798]	7653 [R_{int} = 0.1047]	9020 [R_{int} = 0.1048]	7555 [R_{int} = 0.0673]	32878 [R_{int} = 0.0420]	11346 [R_{int} = 0.0687]
Final R indices [$I > 2\sigma(I)$][a]	$R1$ = 0.0651 $wR2$ = 0.1524	$R1$ = 0.0764 $wR2$ = 0.1593	$R1$ = 0.0533 $wR2$ = 0.1285	$R1$ = 0.0574 $wR2$ = 0.1316	$R1$ = 0.0409 $wR2$ = 0.1345	$R1$ = 0.0436 $wR2$ = 0.0927

[a] $R1 = \Sigma||F_o| - |F_c||/\Sigma|F_o|$, $wR2 = [\Sigma w(F_o^2 - F_c^2)^2/\Sigma w(F_o^2)^2]^{1/2}$ ($w = 1/\sigma^2$).

Table 2 Selected bond distances (Å) and angles (°) in the cations $[M(P4)_2]^{2+}$

1a		**2a**		**1b**		**2b**	
Pd1–P1	2.350(1)	Pt1–P1	2.336(2)	Pd1–P1	2.352(1)	Pt–P1	2.339(1)
P1–C1	1.812(4)	P2–C2	1.815(7)	P1–C1	1.815(4)	P1–C1	1.815(4)
S1–C1	1.748(4)	S1–C1	1.744(7)	S1–C1	1.752(4)	S1–C1	1.749(4)
S1–C3	1.769(4)	S1–C3	1.765(7)	S1–C3	1.770(4)	S1–C3	1.768(4)
C1–C2	1.342(6)	C1–C2	1.340(10)	C1–C1a	1.346(9)	C1–C1a	1.351(10)
C3–C4	1.338(5)	C3–C4	1.337(9)	C3–C4	1.358(9)	C3–C4	1.348(10)
P1–C13	1.816(4)	P2–C40	1.813(7)	P1–C20	1.806(4)	P1–C11	1.814(5)
P1–Pd1–P2	94.72(3)	P1–Pt1–P2	94.53(6)	P1–Pd1–P1a	94.73(6)	P1–Pt–P1a	94.64(6)
C13–P1–C12	109.0(2)	C30–P2–C40	108.7(3)	C10–P1–C20	109.4(2)	C21–P1–C11	108.6(2)
C12–P1–C1	106.4(2)	C30–P2–C2	106.6(3)	C10–P1–C1	104.7(2)	C21–P1–C1	105.0(2)
C49–P4–C43	103.0(2)	C80–P4–C70	102.9(3)	C50–P3–C60	103.4(3)	C61–P3–C51	103.8(3)
C49–P4–C5	99.4(2)	C80–P4–C6	100.1(4)	C5–P3–C50	104.4(2)	C51–P3–C6	104.3(3)

to the formation of two different solvates, namely $[M(P4)_2][BF_4]_2$·2(CH_2Cl_2) (M = Pd (**1a**); Pt (**2a**)) and $[M(P4)_2][BF_4]_2$·2(CH_2Cl_2)·4(C_7H_8) (M = Pd (**1b**); Pt (**2b**)).

$[M(o\text{-}P2)_2][BF_4]$ (M = Ag (3); Cu (4)). Unlike the divergent tetraphosphine ligand P4, o-P2 is a mono-chelating ligand that cannot form extended arrays. Several square-planar complexes with o-P2 have been reported, *e.g.*, NiX_2(o-P2) and $[Rh(o\text{-}P2)_2]^+$.[8] In the latter case, the two o-P2 TTF ligands do not communicate through the Rh(I) center as judged by electrochemistry. In order to further generalize these studies with TTF phosphines we have performed reactions of o-P2 with Ag(I) and Cu(I) to see if such metals in a tetrahedral geometry would induce better communication between the ligands. Syntheses of the tetrahedral complexes were carried out by adding solutions of o-P2 in CH_2Cl_2 to MBF_4 (M = Ag or Cu) salts in CH_3CN to give red-orange solutions. Upon concentration, red-orange crystals were obtained for both Ag and Cu. Analysis of $[Ag(o\text{-}P2)_2][BF_4]$, **3**, by $^{31}P\{^1H\}$ NMR spectroscopy revealed two doublets centered at −1.6 ppm (d, $J_{^{31}P^{109}Ag} = 267$, $J_{^{31}P^{107}Ag} = 236$ Hz) that are similar to the spectra exhibited for other four-coordinate Ag(I) complexes with chelating phosphines such as $[Ag(dppey)_2][NO_3]$ (1.5 ppm, $J_{^{31}P^{109}Ag} = 271$, $J_{^{31}P^{107}Ag} = 235$ Hz) (dppey = $(C_6H_5)_2PCH{=}CHP(C_6H_5)_2$).[14] Solution characterization of $[Cu(o\text{-}P2)_2][BF_4]$, **4**, by $^{31}P\{^1H\}$ NMR spectroscopy revealed a broad feature at +4.40 ppm. The resonances for both products are shifted downfield from the signal for free o-P2 which appears at −18.8 ppm.[8]

X-Ray crystallographic studies

Key crystallographic parameters for compounds **1a**, **1b**, **2a**, **2b**, **3**·1.68(CH_3CN)·0.24(CH_2Cl_2) and **4**·2(CH_3CN) are listed in Table 1.

$[Pd(P4)_2][BF_4]_2$·2(CH_2Cl_2) (1a) and $[Pd(P4)_2][BF_4]_2$·2(CH_2Cl_2)·4(C_7H_8) (1b). The structures of the cations in $[Pd(P4)_2][BF_4]_2$·2(CH_2Cl_2) (**1a**) and $[Pd(P4)_2][BF_4]_2$·2(CH_2Cl_2)·4(C_7H_8) (**1b**) are shown in Fig. 2a and b. Selected bond distances and angles are listed in Table 2. The cation in **1a** exhibits a 27° fold along the S···S axis of the dithiole ring of the TTF, reminiscent of that observed in the cation $[Rh(o\text{-}P2)_2]^+$ which exhibits a bend resulting from close intermolecular interactions between the outer dithiole rings of neighboring TTF units.[8] Folds along the dithiole axis in neutral TTF derivatives are not unusual.[15,16] In fact, density functional calculations reported by Orti and coworkers suggest that the boat conformation of neutral TTF is energetically favored by 2.2 kcal over the planar orientation.[17] Furthermore, gas phase studies performed on the neutral TTF molecule point to the boat form as being more stable than the planar or other bent conformations.[18] Both the planar and boat forms have been experimentally observed in different polymorphs of TTM-TTF (tetra(methylthio)tetrathiafulvalene).[16] In the new P4 derivatives, changes in the TTF conformation are also observed as illustrated by our isolation of **1b** from a mixture of toluene and dichloromethane. This solvate crystallizes with planar TTF

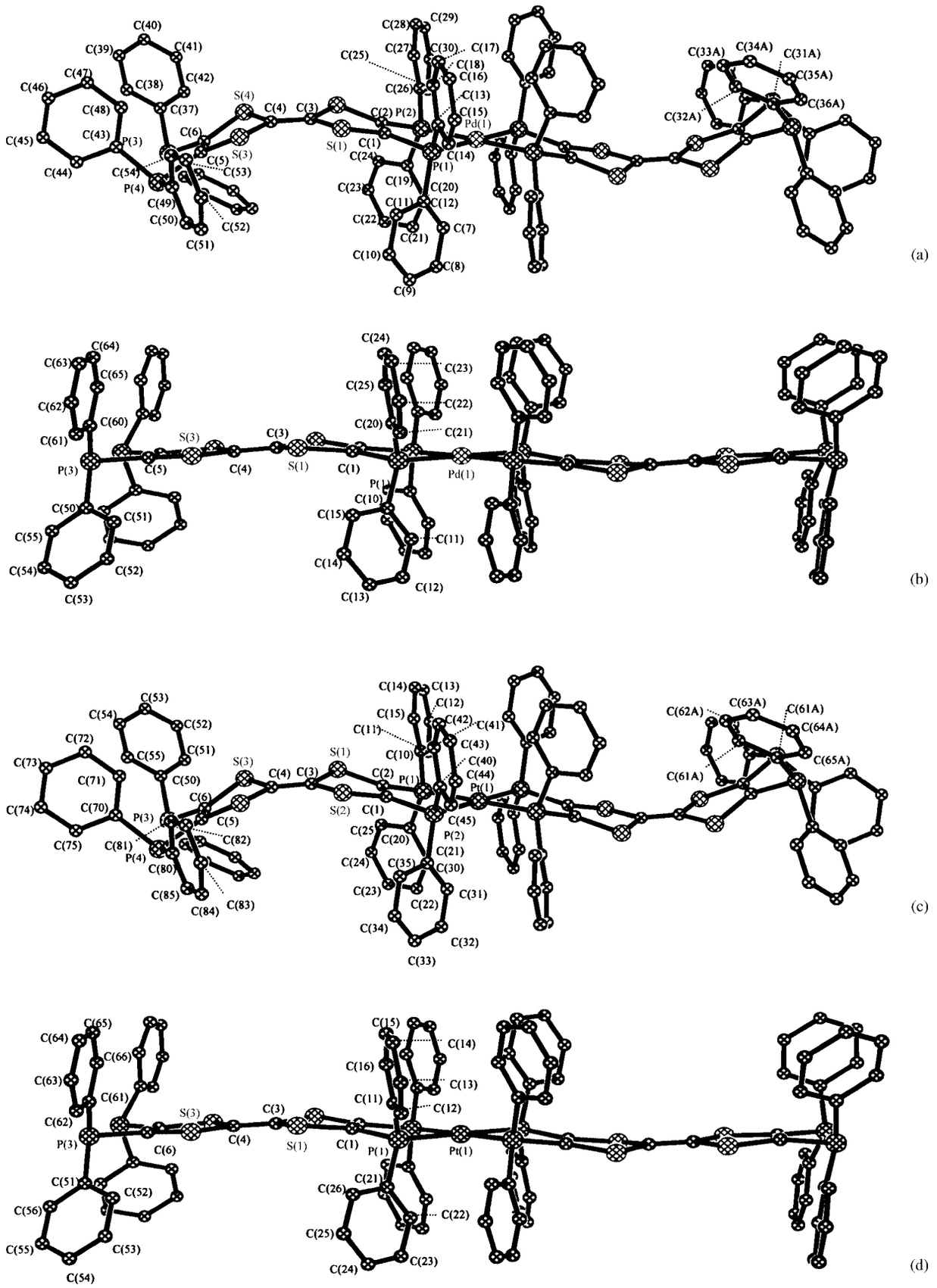

Fig. 2 Labeled diagrams of the cations in (a) **1a**, (b) **1b**, (c) **2a**, and (d) **2b**.

backbones in the ligands and contains interstitial toluene and CH_2Cl_2 molecules. The cations in **1b** assemble in rows separated by CH_2Cl_2 molecules located between the dangling phosphine groups. The arrangement of these rows of cations produces channels where the $[BF_4]^-$ anions and toluene of crystallization reside. The proximity of the interstitial toluene to the phenyl groups located on the two P4 ligands as well as the presence of the CH_2Cl_2 molecules situated between the dangling phosphine groups appear to be influencing the conformation of the TTF backbone. Evidently, subtle variations in weak packing forces are of sufficient energy to alter the degree of bending in the TTF unit (Fig. 3).

$[Pt(P4)_2][BF_4]_2\cdot 2(CH_2Cl_2)$ (2a) and $[Pt(P4)_2][BF_4]_2\cdot 2(CH_2Cl_2)\cdot 4(C_7H_8)$ (2b). Remarkably, when the identity of the metal ion in these Pd compounds is changed to Pt, the same two solvate crystals are obtained. The compounds $[Pt(P4)_2][BF_4]_2\cdot 2(CH_2Cl_2)$ (**2a**) and $[Pt(P4)_2][BF_4]_2\cdot 2(CH_2Cl_2)\cdot 4(C_7H_8)$ (**2b**) are isomorphous with their Pd counterparts (Fig. 2c and d). In fact, the bond lengths within the cations do not vary significantly between the two sets of metal complexes (Table 2). These results indicate that the conformational energy barriers for the TTF groups on these phosphine ligands are very low. The fact that the crystallization conditions are specifically involved in dictating the TTF conformations is evidenced by the startling similarity of the Pd and Pt solvate crystals grown from the same solvents.

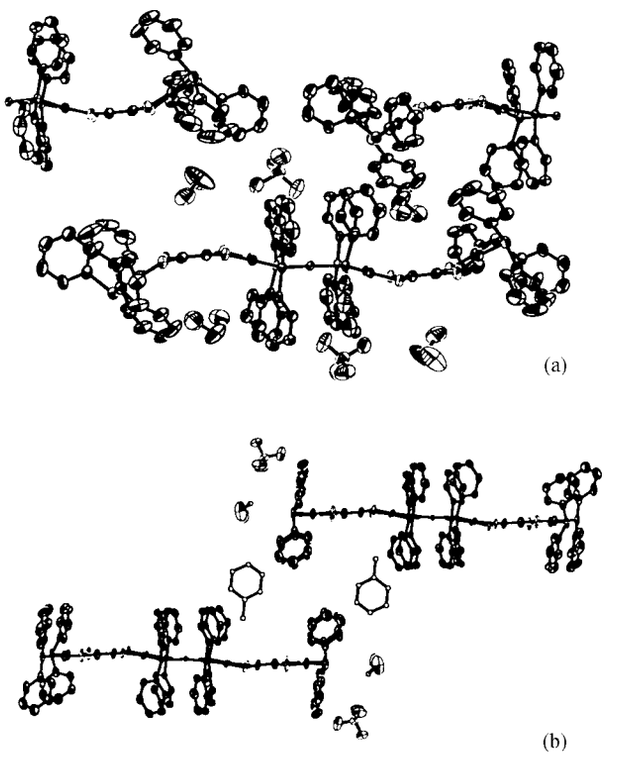

Fig. 3 Packing diagrams with atoms represented at the 50% thermal ellipsoid probability level of (a) **1a** and (b) **1b** with interstitial toluene shown. $[BF_4]^-$ and disordered toluene have been omitted for the sake of clarity.

$[Ag(o\text{-}P2)_2][BF_4]\cdot 1.68(CH_3CN)\cdot 0.24(CH_2Cl_2)$ (3·1.68(CH_3CN)·0.24(CH_2Cl_2)) and $[Cu(o\text{-}P2)_2][BF_4]\cdot 2(CH_3CN)$ (4·2(CH_3CN)). Similar bent and planar conformations of TTF are also observed in the crystal packing arrangements of $[Ag(o\text{-}P2)_2]^+$ and $[Cu(o\text{-}P2)_2]^+$ (Fig. 4). Red-orange, X-ray quality crystals of $[Ag(o\text{-}P2)_2][BF_4]$ (**3**) and $[Cu(o\text{-}P2)_2][BF_4]$ (**4**) were grown by slow evaporation of the respective mother liquids. As shown in Fig. 4, the metal ion in these compounds occupies the center of a distorted tetrahedron. The chelating o-P2 ligands form 5-membered rings with P–M–P angles of 84–86° for Ag and ≈90° for Cu (Table 3). As in the P4 compounds, the TTF backbone is affected by intermolecular interactions, but of a different nature than those found in crystals of **1** and **2**. In order to appreciate the packing arrangements of the molecules in the solvates of **3** and **4**, it is important to remember that TTF is well known to exhibit intermolecular interactions between the sulfur atoms. The packing of TTF containing compounds is significantly affected by these interactions. As one might anticipate, the less sterically encumbered TTF of the o-P2 ligand, unlike the P4 ligand with its four $-PPh_2$ substituents, can participate in S···S interactions; indeed this was observed in our earlier

Table 3 Selected bond distances (Å) and angles (°) in the cations $[M(o\text{-}P2)_2]^+$ in **3**·1.68(CH_3CN)·0.24(CH_2Cl_2) and **4**·2(CH_3CN)

$[Ag(o\text{-}P2)_2]^+$		$[Cu(o\text{-}P2)_2]^+$	
Ag–P1	2.5118(9)	Cu–P1	2.2953(13)
Ag–P2	2.5013(9)	Cu–P2	2.2923(12)
Ag–P3	2.4933(8)	Cu–P3	2.2978(13)
Ag–P4	2.5184(10)	Cu–P4	2.2938(11)
P1–C1	1.832(3)	P1–C1	1.825(4)
S1–C1	1.763(3)	S1–C1	1.757(4)
S1–C3	1.759(3)	S1–C3	1.771(4)
C1–C2	1.349(4)	C1–C2	1.340(5)
C3–C4	1.346(4)	C3–C4	1.346(5)
P1–C17	1.825(3)	P1–C21	1.819(4)
P1–Ag–P2	84.65(2)	P1–Cu–P2	90.38(4)
P3–Ag–P4	84.61(3)	P3–Cu–P4	90.47(4)
P2–Ag–P4	117.40(4)	P2–Cu–P4	130.73(4)
P1–Ag–P4	113.48(3)	P1–Cu–P4	111.41(5)

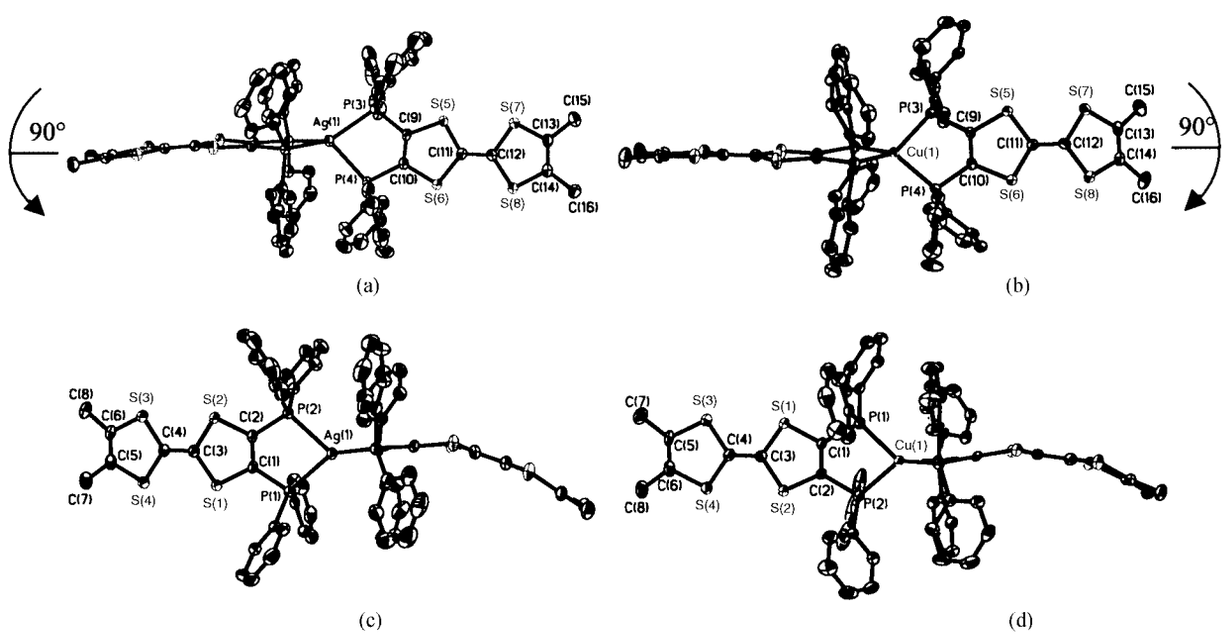

Fig. 4 Thermal ellipsoid plots at the 50% level for $[Ag(o\text{-}P2)_2]^+$ and $[Cu(o\text{-}P2)_2]^+$, emphasizing the flat (a, b) and bent (c, d) conformations of the o-P2 ligands.

Table 4 Cyclic voltammetric data for P4 and related metal complexes (V *vs.* Ag/AgCl, Pt disk electrode in 0.1 M [*n*-Bu_4N][PF_6]/CH_2Cl_2 at a scan rate of 100 mV s^{-1})

Donor	$E^1_{1/2}$	$E^2_{1/2}$	Ref.
P4	0.46	0.86	7
{[Pd(P4)][BF_4]$_2$}$_n$	$E^1_{(anodic)}$ = 1.07		7
[Pd(P4)$_2$][BF_4]$_2$	$E^1_{(anodic)}$ = 0.79		This work
[Pt(P4)$_2$][BF_4]$_2$	$E^1_{(anodic)}$ = 0.82		This work

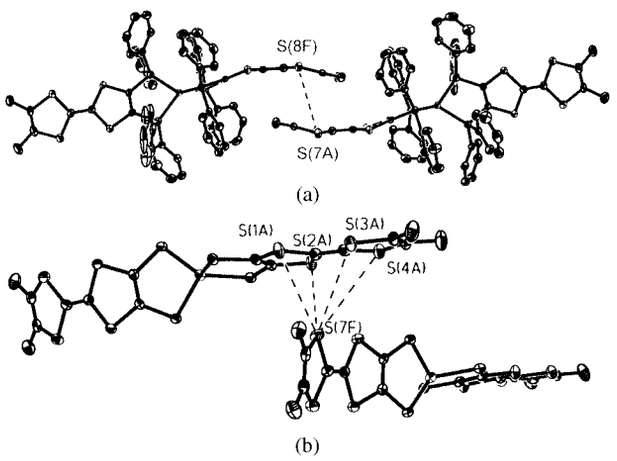

Fig. 5 Thermal ellipsoid plots (50% probability) for $[Cu(o\text{-}P2)_2]^+$ with emphasis on (a) the intermolecular S(7A)···S(8F) distance (4.4 Å) between the boat conformation of the TTF backbones and (b) the intermolecular distance between planar and boat conformations of the TTF backbone (phenyl groups omitted for clarity) selected bond distances (in Å) S(7F)–S(3A) 4.4, S(7F)–S(1A) 3.9, S(7F)–S(2A) 3.8, S(7F)–S(4A) 4.5.

work on [Rh(o-P2)$_2$][BF_4]$_2$.[8] The solid-state packing of the Ag and Cu complexes, however, revealed some unexpected features. One o-P2 ligand assumes a boat conformation with dihedral angles of the S···S axes in the two rings of 24.12(11)° and 14.67(11)° for **3** and 18.70(14)° and 18.09(13)° for **4**, while the TTF in the other o-P2 ligand adopts a planar conformation. These two orientations can best be understood by examining the sulfur–sulfur bond distances between neighboring TTF molecules. In both **3** and **4**, the bent conformation occurs with the outer dithiole ring of each TTF unit assuming a position directly opposite the outer dithiole ring of another TTF moiety (Fig. 5a). The bend is presumably driven by the onset of closer S···S contacts (4.25 Å in **3** and 4.41 Å in **4**). Although these values are longer than the sum of the van der Waals radii for two S atoms (3.8 Å), they are well within the energies for attractive interactions.[19] The planarity of the TTF group in the second o-P2 can also be understood on the basis of favorable S···S contacts. The planar TTF unit of one $[M(o\text{-}P2)_2]^+$ cation is situated directly below the outer dithiole ring of a neighboring cation such that all four S atoms on the planar TTF experience good contacts with the next S (Fig. 5b). Sulfur–sulfur separations range from 3.8–4.5 Å and are shorter on the average than those observed for two bent dithiole rings. Unlike the P4 complexes, whose crystallization appears to be controlled by solvent interactions, the solid-state structures of the o-P2 compounds are clearly dependent on intermolecular S···S interactions.

Electrochemical studies

Cyclic voltammetric studies of **1** and **2** revealed that they exhibit quite similar electrochemical behavior, *viz.*, one irreversible oxidation that occurs at more positive potentials than the two reversible oxidations exhibited by the free ligand (Table 4). There is also a reversible reduction in these compounds that occurs at $E_{1/2}$(red) = −0.38 V for **1** and −0.45 V for **2**.

Table 5 Cyclic voltammetric data for o-P2 and various metal complexes (V *vs.* Ag/AgCl, Pt disk electrode in 0.1 M [*n*-Bu_4N][PF_6]/CH_2Cl_2 at a scan rate of 100 mV s^{-1})

Donor	$E^1_{1/2}$	$E^2_{1/2}$	Ref.
o-P2	0.41	0.85	7
[Rh(o-P2)$_2$][BF_4]	0.62	1.01	8
[Ag(o-P2)$_2$][BF_4]	0.55	0.97	This work
[Cu(o-P2)$_2$][BF_4]	0.53	0.97	This work

Unlike the irreversible electrochemistry of the P4 compounds **1** and **2**, the o-P2 compounds **3** and **4** exhibit two reversible oxidations (Table 5). These are shifted to more positive potentials than the unbound ligand as expected.[8] The first oxidation is still quite accessible, however, as evidenced by the fact that reactions of the compounds with $AgBF_4$ or tris(*p*-bromophenyl)amminium tetrafluoroborate lead to the immediate formation of dark green solutions, an indication of the presence of the radical TTF chromophore. EPR spectral analysis revealed isotropic signals near $g = 2$ for both the Ag and Cu complexes. The fact that there are only two oxidations rather than four for the two o-P2 ligands in these complexes reflects a lack of electronic communication between the two π-systems, *i.e.*, the mixed valence compounds are not stable.

Experimental

Unless otherwise noted, all procedures were performed under a dry nitrogen atmosphere using standard Schlenk-line techniques. Solvents were freshly distilled under N_2 immediately before use. Acetonitrile was distilled from 3 Å sieves, dichloromethane was distilled over P_2O_5, and diethyl ether and toluene were distilled from Na–K amalgam. $^{31}P\{^1H\}$ NMR spectra were referenced to H_3PO_4 and performed on a Unity Plus 300 spectrometer at 121 MHz. EPR spectra were performed on an ESP 300E Bruker with an Oxford cryostat ESR900. Cyclic voltammetry experiments were carried out on a CH Instruments Electrochemical Analyzer in 0.1 M [*n*-Bu_4N][PF_6]/CH_2Cl_2 at a Pt disk working electrode with a Ag/AgCl reference and a Pt counter electrode.

Syntheses

[Pd(P4)$_2$][BF_4]$_2$ (1). [Pd(NCMe)$_4$][BF_4]$_2$ (48.6 mg, 0.110 mmol) was suspended in 5 mL of CH_2Cl_2, and P4 (526 mg, 0.559 mmol) was dissolved in 15 mL of CH_2Cl_2. The suspension of [Pd(NCMe)$_4$][BF_4]$_2$ was slowly added *via* cannula to the P4 solution to yield a dark red-orange solution. After 15 minutes, toluene (60 mL) was added, and the solution was condensed to a lower volume (≈50 mL) followed by heating to 100 °C to give an orange solution and a brown solid. The crude brown solid was collected by suction filtration in air and extracted with CH_2Cl_2 (20 mL) to separate the desired product from an insoluble material (presumably oligomeric). The CH_2Cl_2 extract was treated with 40 mL of toluene, and the process of reducing the volume and heating was repeated. The entire process was carried out a third time and hexanes was added to yield 34.2 mg, 14.4%, of a brown solid. $^{31}P\{^1H\}$ NMR (CH_2Cl_2) +41.6, −18.0 ppm.

[Pt(P4)$_2$][BF_4]$_2$ (2). A method similar to the [Pd(P4)$_2$][BF_4]$_2$ synthesis was used. [Pt(NCMe)$_4$][BF_4]$_2$ (29.3 mg, 0.055 mmol) and P4 (415.7 mg, 0.432 mmol) were dissolved in the manner described above to form a red solution that, after precipitation with Et_2O, yielded 27.2 mg, 22%, of a red solid. $^{31}P\{^1H\}$ NMR (CH_2Cl_2) +32.6 (J_{Pt-P} = 1201 Hz) and −18.0 ppm.

[Ag(o-P2)$_2$][BF_4] (3). Separate flasks were charged with one equivalent of $AgBF_4$ (11.3 mg, 0.058 mmol) in 10 mL of MeCN (colorless) and two equivalents of o-P2 (59.7 mg, 0.10 mmol) in

10 mL of CH_2Cl_2 (pale orange). The o-P2 solution was added to the stirring solution of $AgBF_4$ which effected a color change to orange-red within 5 min. The solution was condensed to ≈20% of the original volume during which time X-ray quality crystals formed. After further condensation, the product was washed with copious amounts of Et_2O and dried *in vacuo* to yield 65.3 mg, 94%, of an orange-red solid. $^{31}P\{^1H\}$ NMR (CD_3CN, CH_2Cl_2) −1.6 (dd, J_{Ag-P} = 134, J_{Ag-P} = 118 Hz).

[Cu(o-P2)$_2$][BF$_4$] (4). A method similar to the [Ag(o-P2)$_2$][BF$_4$] synthesis outlined above was used. [Cu(NCMe)$_4$][BF$_4$] (26.5 mg, 0.0842 mmol) in 10 mL of MeCN and o-P2 (101.3 mg, 0.1686 mmol) in 10 mL of CH_2Cl_2 were combined to form an red-orange solution. The solution was condensed to dryness to yield a mixture of red crystals and red-orange powder. The product was redissolved in 10 mL of CH_2Cl_2, and a red-orange solid was precipitated with 40 mL of Et_2O. The solid was rinsed with Et_2O until the washings became colorless and then dried *in vacuo*. The yield was 91 mg, 80%. $^{31}P\{^1H\}$ NMR (CD_3CN, CH_2Cl_2) 4.4 ppm.

X-Ray crystallographic details and structure solution

For all compounds, the data were collected on a Siemens SMART CCD diffractometer at 173 ± 2 K (**1a**, **1b**, **2a**, **2b**, **3**·1.68(CH_3CN)·0.24(CH_2Cl_2)) or 110 ± 2 K (**4**·2(CH_3CN)) with graphite monochromated Mo-Kα (λ = 0.71073 Å) radiation. The data were corrected for Lorentz and polarization effects. The frames were integrated with the Siemens SAINT[20] software package, and the data were corrected for absorption using the SADABS program.[21] The structures were solved by direct methods by the use of the SHELXS-97[22] program in the Bruker SHELXTL v5.1 software package.[23] All non-hydrogen atoms were refined with anisotropic thermal parameters by full matrix least squares calculations on F^2 using the SHELXL-97 program.[24] Hydrogen atoms were inserted at calculated positions and constrained with isotropic thermal parameters. Crystallographic parameters are listed in Table 1 with any special refinement conditions noted in the following paragraphs.

CCDC reference number 186/1880.

See http://www.rsc.org/suppdata/dt/a9/a908559i/ for crystallographic files in .cif format.

[Pd(P4)$_2$][BF$_4$]$_2$·2(CH_2Cl_2), (1a). Brown crystals suitable for single crystal X-ray analysis were grown by slow diffusion of hexanes into CH_2Cl_2 solutions of [Pd(P4)$_2$][BF$_4$]$_2$, mounted in inert oil, and transferred to the cold stream of the diffractometer.

[Pt(P4)$_2$][BF$_4$]$_2$·2(CH_2Cl_2), (2a). Red crystals suitable for single crystal X-ray analysis were grown by slow diffusion of hexanes into CH_2Cl_2 solutions of [Pt(P4)$_2$][BF$_4$]$_2$. A crystal was coated in oil and transferred to the cold stream of the diffractometer.

[Pd(P4)$_2$][BF$_4$]$_2$·2(CH_2Cl_2)·4(C_7H_8), (1b) and [Pt(P4)$_2$][BF$_4$]$_2$·2(CH_2Cl_2)·4(C_7H_8), (2b). Brown (Pd) and red (Pt) crystals of the compounds suitable for single crystal X-ray analysis were grown by slow diffusion of toluene into CH_2Cl_2 solutions of [M(P4)$_2$][BF$_4$]$_2$. Suitable specimens were mounted in inert oil and transferred to the cold stream of the diffractometer. Both structures were refined in the *C*2 space group with the use of Platon v. 80399 to add missing symmetry.[25] Two disordered toluene molecules on special positions were modeled isotropically with restraints on bond distances and angles.

[Ag(o-P2)$_2$][BF$_4$]·1.68(CH_3CN)·0.24(CH_2Cl_2), (3·1.68(CH_3CN)·0.24(CH_2Cl_2)). A red-orange crystal of the complex grown by concentration of the mother liquid was secured on the tip of a glass fiber with Dow Corning grease and transferred to the cold N_2 stream of the diffractometer. The data were refined in the program SHELXH.[26] The asymmetric unit contains two independent [Ag(o-P2)$_2$][BF$_4$] units, three fully occupied acetonitrile molecules (two of which are disordered), and a region that contains disordered dichloromethane and acetonitrile molecules. Both partially occupied molecules were modeled with restraints on the bond distances and angles.

[Cu(o-P2)$_2$][BF$_4$]·2(CH_3CN), (4·2(CH_3CN)). Red-orange crystals of the Cu complex were grown by slow evaporation of the mother liquid. The crystal selected for study was mounted on the end of a glass fiber with Dow Corning grease and transferred to the cold N_2 stream (110 ± 2 K) of the diffractometer.

Acknowledgments

We gratefully acknowledge ACS-PRF for providing financial support, Dr Marc Fourmigué for supplying o-P2, Dr Rodolphe Clérac for the EPR measurements, and Dr Donald Ward and Dr Xiang Ouyang for help with the X-ray crystallography.

References

1 J. M. Manriquez, G. T. Yee, R. S. McLean, A. J. Epstein and J. S. Miller, *Science*, 1991, **252**, 1415; Y. Pei, O. Kahn, K. Nakatani, E. Codjovi, C. Mathonière and J. Sletten, *J. Am. Chem. Soc.*, 1991, **113**, 6558; J. P. Cornelissen, R. Le Loux, J. Jansen, J. G. Haasnoot, J. Reedijk, E. Horn, A. L. Spek, B. Pomarède, J. P. Legros and D. Reefman, *J. Chem. Soc., Dalton Trans.*, 1992, 2911; S. Serroni, G. Denti, S. Campagna, A. Juris, M. Ciano and V. Balzani, *Angew. Chem., Int. Ed. Engl.*, 1992, **31**, 1493; C. Kollmar and O. Kahn, *Acc. Chem. Res.*, 1993, **26**, 259; J. S. Miller and A. J. Epstein, *Angew. Chem., Int. Ed. Engl.*, 1994, **33**, 385; O. Kahn, in *Molecular Magnetism*, New York, VCH, 1993; B. Pomarède, B. Garreau, I. Malfante, L. Valade, P. Cassoux, J. P. Legros, A. Audouard, L. Brossard, J. P. Ulmet, M. L. Doublet and E. Canadell, *Inorg. Chem.*, 1994, **33**, 3401; H. O. Stumpf, Y. Pei, C. Michaut, O. Kahn, J. R. Renard and L. Ouahab, *Chem. Mater.*, 1994, **6**, 257; W. Kaim and M. Moscherosch, *Coord. Chem. Rev.*, 1994, **129**, 157.

2 G. Saito and S. Kagoshima, eds., *The Physics and Chemistry of Organic Superconductors*, Springer, Berlin, 1990; F. Wudl, *Acc. Chem. Res.*, 1984, **17**, 227; J. M. Williams, H. H. Wang, T. J. Emge, U. Geiser, M. A. Beno, P. C. W. Leung, K. D. Carlson, R. J. Thorn, A. J. Schultz and M. H. Whangbo, *Prog. Inorg. Chem.*, ed. S. J. Lippard, Wiley, New York 1987, vol. 35, pp. 51–218.

3 A. Davidson, K. Boubekeur, A. Pénicaud, P. Auban, C. Lenoir, P. Batail and G. Hervé, *J. Chem. Soc., Chem. Commun.*, 1989, 1373; A. Pénicaud, K. Boubekeur, P. Batail, E. Canadell, P. Auban-Senzier and D. Jérome, *J. Am. Chem. Soc.*, 1993, **115**, 4101; C. Coulon, C. Livage, L. Gonzalvez, K. Boubekeur and P. Batail, *J. Phys. I*, 1993, **3**, 1; E. Coronado and C. J. Gómez-García, *Comments Inorg. Chem.*, 1995, **17**, 255; C. J. Gómez-García, C. Giménez-Saiz, S. Triki, E. Coronado, P. L. Magueres, L. Ouahab, L. Ducasse, C. Sourisseau and P. Delhaes, *Inorg. Chem.*, 1995, **34**, 4139; J. R. Galán-Mascarós, C. Giménez-Saiz, S. Triki, C. J. Gómez-García, E. Coronado and L. Ouahab, *Angew. Chem., Int. Ed. Engl.*, 1995, **34**, 1460; E. Coronado, J. R. Galán-Mascarós, C. Giménez-Saiz, C. J. Gómez-García and S. Triki, *J. Am. Chem. Soc.*, 1998, **120**, 4671; H. Kobayashi, H. Tomita, T. Naito, A. Kobayashi, F. Sakai, T. Watanabe and P. Cassoux, *J. Am. Chem. Soc.*, 1996, **118**, 368.

4 M. Kurmoo, A. W. Graham, P. Day, S. J. Coles, M. B. Hursthouse, J. L. Caulfield, J. Singleton, F. L. Pratt, W. Hayes, L. Ducasse and P. Guionneau, *J. Am. Chem. Soc.*, 1995, **117**, 12209.

5 A. Aumüller, P. Erk, G. Klebe, S. Hünig, J. U. von Schütz and H.-P. Werner, *Angew. Chem., Int. Ed. Engl.*, 1986, **8**, 740; R. Kato, H. Kobayashi and A. Kobayashi, *J. Am. Chem. Soc.*, 1989, **111**, 5224; N. Le Narvor, N. Robertson, E. Wallace, J. D. Kilburn, A. E. Underhill, P. N. Bartlett and M. Webster, *J. Chem. Soc., Dalton Trans.*, 1996, 823; J. Ramos, C. J. Gómez-García, E. Coronado and P. Delhaès, *Synth. Met.*, 1997, **86**, 1807; K. R. Dunbar, *Angew. Chem., Int. Ed. Engl.*, 1996, **35**, 1659; H. Zhao, R. A. Heintz, R. D. Rogers and K. R. Dunbar, *J. Am. Chem. Soc.*, 1996, **118**, 12844; R. A. Heintz, H. Zhao, X. Ouyang, G. Grandinetti, J. Cowen and K. R. Dunbar, *Inorg. Chem.*, 1999, **38**, 144; H. Zhao, R. A. Heintz, X. Ouyang, K. R. Dunbar, C. F. Campana and R. D. Rogers, *Chem. Mater.*, 1999, **11**, 736.

6 M. Fourmigué and P. Batail, *Bull. Soc. Chim. Fr.*, 1992, **129**, 29; S. Jarchow, M. Fourmigué and P. Batail, *Acta Crystallogr.*, *Sect. C*, 1993, **49**, 1936; M. Fourmigué and Y.-S. Huang, *Organometallics*, 1993, **12**, 797; F. Gerson, A. Lamprecht and M. Fourmigué, *J. Chem. Soc.*, *Perkin Trans. 2*, 1996, 1; J. M. Asara, C. E. Uzelmeier, K. R. Dunbar and J. Allison, *Inorg. Chem.*, 1998, **37**, 1833;
7 C. E. Uzelmeier, PhD Thesis, Michigan State University, 1998; C. E. Uzelmeier, S. L. Bartley, M. Fourmigué, R. Rogers, G. Grandinetti and K. R. Dunbar, *Inorg. Chem.*, 1998, **37**, 6706.
8 M. Fourmigué, C. E. Uzelmeier, K. Boubekeur, S. L. Bartley and K. R. Dunbar, *J. Organomet. Chem.*, 1997, **529**, 343.
9 P.-W. Wang and M. A. Fox, *Inorg. Chem.*, 1994, **33**, 2938.
10 *Comprehensice Coordination Chemistry*, eds. A. C. McAuliffe, G. Wilkinson, R. D. Gillard and J. A. McCleverty, Pergamon, Oxford, 1987, p. 989.
11 G. Pilloni and B. Lonato, *Inorg. Chim. Acta*, 1993, **208**, 17.
12 G. J. Kubas, *Acc. Chem. Res.*, 1988, **12**, 120; J. F. Young, J. A. Osborne, F. H. Jardine and G. Wilkinson, *Chem. Commun.*, 1965, 131; G. J. Kubas, C. J. Unkefer, B. I. Swanson and E. Fukushima, *J. Am. Chem. Soc.*, 1986, **108**, 7000.
13 Due to the tendency of the P4 ligand to form oligomers in the presence of equimolar quantities of metal cations, excess ligand was used to favor the bis P4 products. An insoluble brown side product, presumably an extended array of $[M(P4)[BF_4]_2]_n$, was invariably present. This material which is produced in nearly quantitative yields in CH_3CN significantly reduces the yield of the mononuclear species in spite of the use of excess phosphine.
14 S. J. Berners Price, C. Brevard, A. Pagelot and P. J. Sadler, *Inorg. Chem.*, 1985, **24**, 4278.
15 M. Fourmigué and P. Batail, *J. Chem. Soc.*, *Chem. Commun.*, 1991, **19**, 1370; B. Garreau, D. de Montauzon, P. Cassoux, J.-P. Legros, J.-M. Fabre, K. Saoud and S. Chakroune, *New J. Chem.*, 1995, **19**, 161; J. Ippen, C. Tao-pen, B. Starker, D. Schweitzer and H. A. Staab, *Angew. Chem.*, *Int. Ed. Engl.*, 1980, **19**, 67; H. A. Staab, J. Ippen, C. Tao-pen, C. Krieger and B. Starker, *Angew. Chem.*, *Int. Ed. Engl.*, 1980, **19**, 66; K. Boubekeur, P. Batail, F. Bertho and A. Robert, *Acta Crystallogr.*, *Sect. C*, 1991, **47**, 1109; K. Boubekeur, C. Lenoir, P. Batail, R. Carlier, A. Tallec, M.-P. Le Paillard, D. Lorcy and A. Robert, *Angew. Chem.*, *Int. Ed. Engl.*, 1994, **33**, 1379.
16 C. Katayama, M. Honda, H. Kumagai, J. Tanaka, G. Saito and H. Inokuchi, *Bull. Chem. Soc. Jpn.*, 1985, **58**, 2272; H. Endres, *Z. Naturforsch.*, *Teil B*, 1986, **41**, 1351.
17 R. Viruela, P. M. Viruela, R. Pou-Amérigo and E. Orti, *Synth. Met.*, 1999, **103**, 1991.
18 I. Hargittai, J. Brunvoll, M. Kolonits and V. Khodorkovsky, *J. Mol. Struct.*, 1994, **317**, 273.
19 For a compilation of data on S···S interactions see: A. Ellern, J. Bernstein, J. Y. Becker, S. Zamir and L. Shahal, *Chem. Mater.*, 1994, **6**, 1378 and references therein.
20 SAINT, Program for area detector absorption correction, Siemens Analytical X-Ray Instruments Inc., Madison, WI 53719, USA, 1994–1996.
21 G. M. Sheldrick, SADABS, Program for Siemens area detector absorption correction, University of Göttingen, 1996.
22 G. M. Sheldrick, SHELXS-97, Program for crystal structure determination, University of Göttingen, 1997.
23 G. M. Sheldrick, SHELXTL, An integrated system for solving, refining and displaying crystal structures from diffraction data (Revision 5.1), University of Göttingen, 1985.
24 G. M. Sheldrick, SHELXL-97, Program for refining crystal structures, University of Göttingen, 1997.
25 (*a*) PLATON, A. L. Spek, *Acta Crystallogr.*, *Sect. A*, 1990, **46**, C34; (*b*) PLATON, A multipurpose Crystallographic Tool, Utrecht University, Utrecht, The Netherlands, 1998.
26 G. M. Sheldrick, SHELXH, Program for refining large crystal structures, University of Göttingen, 1997.